Phase noise of whispering gallery photonic hyper-parametric microwave oscillators

Anatoliy A. Savchenkov[1], Enrico Rubiola[1,2,3], Andrey B. Matsko[1], Vladimir S. Ilchenko[1], and Lute Maleki[1,2]

[1] *OEwaves Inc., 1010 East Union St., Pasadena, CA 91106;*
[2] *Jet Propulsion Laboratory, California Institute of Technology, 4800 Oak Grove Drive, Pasadena, California 91109-8099;*
[3] *FEMTO-ST Institute, UMR CNRS 6174 Besançon, France*

Andrey.Matsko@oewaves.com

Abstract: We report on the experimental study of phase noise properties of a high frequency photonic microwave oscillator based on four wave mixing in calcium fluoride whispering gallery mode resonators. Specifically, the oscillator generates ~ 8.5 GHz signals with -120 dBc/Hz at 100 kHz from the carrier. The floor of the phase noise is limited by the shot noise of the signal received at the photodetector. We argue that the performance of the oscillator can be significantly improved if one uses extremely high finesse resonators, increases the input optical power, supersaturates the oscillator, and suppresses the residual stimulated Raman scattering in the resonator. We also disclose a method of extremely sensitive measurement of the integral dispersion of millimeter scale dielectric resonators.

OCIS codes: (230.5750) Resonators; (190.4380) Nonlinear optics, four-wave mixing; (190.4360) Nonlinear optics, devices

References and links

1. K. Hosoya, K. Ohata, M. Funabashi, T. Inoue, and M. Kuzuhara, "V-band HJFET MMIC DROs with low phase noise, high power, and excellent temperature stability," IEEE Trans. Microwave Theory Tech. **51**, 2250-2258 (2003).
2. B. A. Floyd, S. K. Reynolds, U. R. Pfeiffer, T. Zwick, T. Beukema, and B. Gaucher, "SiGe bipolar transceiver circuits operating at 60 GHz," IEEE J. Solid-State Circuits **40**, 156-167 (2005).
3. E. N. Ivanov E. N. and M. E. Tobar, "Low phase-noise microwave oscillators with interferometric signal processing," IEEE Trans. Microwave Theory Tech. **54**, 3284-3294 (2006).
4. J. F. Gravel J. F. and J. S. Wight, "On the conception and analysis of a 12-GHz push-push phase-locked DRO," IEEE Trans. Microwave Theory Tech. **54**, 153-159 (2006).
5. Y. Ji, X. S. Yao, and L. Maleki, "Compact optoelectronic oscillator with ultralow phase noise performance," Electron. Lett. **35**, 1554-1555 (1999).
6. D. Eliyahu, K. Sariri, M. Kamran, and M. Tokhmakhian, "Improving short and long term frequency stability of the opto-electronic oscillator," Proc. IEEE International Frequency Control Symposium, 580-583 (2002).
7. N. Yu, E. Salik, and L. Maleki, "Ultralow-noise mode-locked laser with coupled optoelectronic oscillator configuration," Opt. Lett. **30**, 1231-1233 (2005).
8. J. J. McFerran, E. N. Ivanov, A. Bartels, G. Wilpers, C. W. Oates, S. A. Diddams, and Hollberg, "Low-noise synthesis of microwave signals from an optical source," Electron. Lett. **41**, 650-651 (2005).
9. V. V. Vassiliev, V. L. Velichansky, V. S. Ilchenko, M. L. Gorodetsky, L. Hollberg, and A. V. Yarovitsky, "Narrow-line-width diode laser with a high-Q microsphere resonator," Opt. Commun. **158**, 305312 (1998).
10. A. A. Savchenkov, A. B. Matsko, V. S. Ilchenko, and L. Maleki, "Optical resonators with ten million finesse," Opt. Express **15**, 6768-6773 (2007).

#90022 - $15.00 USD Received 21 Nov 2007; revised 22 Feb 2008; accepted 22 Feb 2008; published 12 Mar 2008

11. A. B. Matsko, A. A. Savchenkov, N. Yu, and L. Maleki, "Whispering-gallery-mode resonators as frequency references: I. Fundamental limitations," J. Opt. Soc. Am. B **24**, 1324-1335 (2007).
12. A. A. Savchenkov, A. B. Matsko, V. S. Ilchenko, N. Yu, and L. Maleki, "Whispering-gallery-mode resonators as frequency references. II. Stabilization," J. Opt. Soc. Am. B **24**, 2988-2997 (2007).
13. T. J. Kippenberg, S. M. Spillane, and K. J. Vahala, "Kerr-Nonlinearity Optical Parametric Oscillation in an Ultrahigh-Q Toroid Microcavity," Phys. Rev. Lett. **93**, 083904 (2004).
14. P. Del Haye, A. Schliesser, O. Arcizet, T. Wilkins, R. Holzwarth, T. J. Kippenberg, "Optical frequency comb generation from a monolithic microresonator," Nature **450**, 1214-1217 (2007).
15. A. B. Matsko, A. A. Savchenkov, V. S. Ilchenko, and L. Maleki, "Nonlinear optics with WGM crystalline resonators: advances and puzzles," 2004 Digest of the LEOS Summer Topical Meeting "WGM Microcavities" (2004).
16. A. A. Savchenkov, A. B. Matsko, D. Strekalov, M. Mohageg, V. S. Ilchenko, and L. Maleki, "Low Threshold Optical Oscillations in a Whispering Gallery Mode CaF_2 Resonator," Phys. Rev. Lett. **93**, 243905 (2004).
17. A. A. Savchenkov, A. B. Matsko, D. Strekalov, M. Mohageg, V. S. Ilchenko, and L. Maleki, "All-optical photonic oscillator with high-Q whispering gallery mode resonators," Proc. IEEE International Topical Meeting on Microwave Photonics, 205-208 (2004).
18. A. B. Matsko, A. A. Savchenkov, D. Strekalov, V. S. Ilchenko, and L. Maleki, "Optical hyper-parametric oscillations in a whispering gallery mode resonator: threshold and phase diffusion," Phys. Rev. A **71**, 033804 (2005).
19. A. B. Matsko, A. A. Savchenkov, D. Strekalov, and L Maleki, "High frequency photonic microwave oscillators based on WGM resonators," 2005 Digest of the LEOS Summer Topical Meetings, 113-114 (2005).
20. D. N. Klyshko, "Photons and Nonlinear Optics" (Taylor and Francis, New York, 1988).
21. M. Haelterman, S. Trillo, and S. Wabnitz, "Additive-modulation-instability ring laser in the normal dispersion regime of a fiber," Opt. Lett. **17**, 745-747 (1992)
22. S. Coen and M. Haelterman, "Modulational instability induced by cavity boundary conditions in a normally dispersive optical fiber," Phys. Rev. Lett. **79**, 4139-4142 (1997).
23. S. Coen and M. Haelterman, "Continuous-wave ultrahigh-repetition-rate pulse-train generation through modulational instability in a passive fiber cavity," Opt. Lett. **26**, 39-41 (2001).
24. E. Rubiola, "Phase noise and frequency stability in oscillators," Cambridge University Press, 2008 (in press). Online abridged version: E. Rubiola, "The Leeson effect – Phase noise in quasilinear oscillators," http://arxiv.org/abs/physics/0502143.
25. D. B. Leeson, "A simple model of feed back oscillator noise spectrum," Proc. IEEE **54**, 329330 (1966).
26. A. L. Schawlow and C. H. Townes, "Infrared and optical masers," Phys. Rev. **112**, 1940-1949 (1958).
27. J. R. Vig (chair.), "IEEE Standard Definitions of Physical Quantities for Fundamental Frequency and Time Metrology–Random Instabilities" (IEEE Standard 1139-1999), IEEE 1999.
28. L. Maleki, A. A. Savchenkov, V. S. Ilchenko, and A. B. Matsko, "Whispering gallery mode lithium niobate micro-resonators for photonics applications," Proc. SPIE **5104** (2003).
29. M. Daimon and A. Masumura, "High-accuracy measurements of the refractive index and its temperature coefficient of calcium fluoride in a wide wavelength range from 138 to 2326 nm," Appl. Opt. **41**, 5275-5281 (2002).

1. Introduction

High frequency low-noise microwave signals are required in various applications including high performance communication and radar systems. The signals are usually produced electronically by multiplying the frequency of quartz oscillators or are generated directly using microwave cavities [1]-[4]. Photonic techniques for generation of microwave signals provide an alternative solutions, adding new features to the microwave oscillators, such as ultra-low phase noise and small size [5]-[8]. Furthermore, photonic devices are potentially able to achieve low phase noise for high frequency (exceeding 30 GHz) microwave signals, while the performance of electronic devices gradually degrades with the frequency increase [1]. In this paper we focus on microwave photonic sources that utilize optical whispering gallery mode (WGM) resonators and their nonlinear properties. The resonators are characterized with very-high Q, are compact as well as environmentally stable, and are promising for fabrication of miniature high performance microwave photonic oscillators.

Photonic microwave oscillators are generally based on generation and subsequent demodulation of polychromatic light to produce a well defined and stable beat-note signal. There are several approaches for realization of the oscilators. The most obvious way is based on stabilization of two lasers using different modes of the same optical resonator. This technique was

#90022 - $15.00 USD Received 21 Nov 2007; revised 22 Feb 2008; accepted 22 Feb 2008; published 12 Mar 2008

used, for instance, in proof of the principle experiments with fused silica WGM resonator stabilized diode lasers [9]. Crystalline WGM resonators seem to be more suitable for this purpose because of their high Q-factors [10] as well as potentially high stability [11, 12]. Another way for generation of coherent optical signals is based on excitation of hyperparametric oscillations in WGM resonators [13]-[19]. Such an oscillator has the advantage of a small size, and low input power, and can generate microwave signals at any desired frequency, which is determined by the size of the resonator. Study of properties of such an oscillator is the theme of this paper.

Hyperparametric optical oscillation [20] is based on four-wave mixing among two pump, signal, and idler photons, and results in the growth of the signal and idler optical sidebands from vacuum fluctuations at the expense of the pumping wave. Hyperparametric oscillations are different from the parametric ones. Parametric oscillations are based on a $\chi^{(2)}$ nonlinearity coupling three photons and have phase matching conditions involving far separated optical frequencies. By contrast, the hyperparametric oscillations are based on a $\chi^{(3)}$ nonlinearity coupling four photons and have phase matching conditions involving nearly-degenerate optical frequencies.

The hyperparametric oscillator based on WGM modes is fundamentally identical to the additive modulational instability ring laser predicted and demonstrated in the fiber ring resonators [21, 22, 23]. The basic difference between these systems is the intrinsic suppression of the Brillouin scattering (generally present in the fiber lasers) and the presence of a significant geometrical dispersion in WGM resonators of the proper size.

A high intracavity intensity in high finesse WGMs results in $\chi^{(3)}$ based four-photon processes like $\hbar\omega + \hbar\omega \rightarrow \hbar(\omega + \omega_M) + \hbar(\omega - \omega_M)$, where ω is the carrier frequency of the external pumping, and ω_M is determined by the the free spectral range of the resonator $\omega_M \approx \Omega_{FSR}$. Cascading of the process and generating multiple equidistant signal and idler harmonics (optical comb) is also possible in this oscillator [14]. Demodulation of the oscillator output by means of a fast photodiode results in the generation of high frequency microwave signals at frequency ω_M. The spectral purity of the signal increases with increasing Q factor of the WGMs and the optical power of the generated signal and idler. The pumping threshold value of the oscillation can be as small as several microWatt for the resonators with ultrahigh Q-factors [18].

Here we report on the experimental realization of a low noise hyper-parametric microwave photonic oscillator based on a calcium fluoride WGM resonator. The oscillator produces signals at 8.4 GHz with a phase noise of -120 dBc/Hz at 100 kHz from the carrier, while consuming less than 100 mW of optical power at 1319 nm. We show that, as expected, the noise floor of the oscillator is given by the optical shot noise. The number of generated optical harmonics in our oscillator is restricted due to the stimulated Raman scattering, which, if present, adds noise to the generated microwave signal. We also discuss possible ways of increasing the number of the signal and idler sidebands to create an optical combs [14] for generation of low phase noise microwave signals [8].

The paper is organized as follows. We theoretically study the phase noise of the oscillator in Section II, followed by the experimental results presented in Section III. In Section IV we describe the dispersive properties of the WGM resonators as relates to the generation of an optical comb and report on our measurement of the dispersion in a calcium fluoride resonator. Possible ways of improvement of the oscillator performance are presented in Section V.

2. Theory

2.1. General properties of the hyperparametric oscillations

Let us analyze the scheme shown in Fig. 1 to explain the basic classical properties of the hyperparametric oscillator based on a continuously pumped nonlinear WGM resonator. The solid state WGM resonator is presented as a ring cavity containing localized in space lossless Kerr

#90022 - $15.00 USD Received 21 Nov 2007; revised 22 Feb 2008; accepted 22 Feb 2008; published 12 Mar 2008

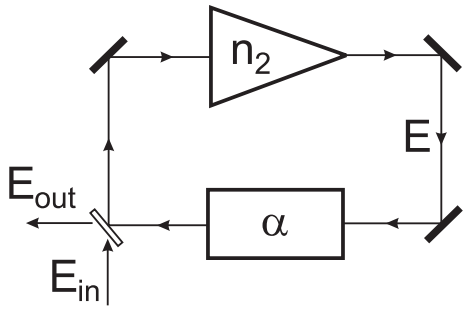

Fig. 1. A model of a WGM based hyperparametric oscillator. The ring resonator contains a lossless Kerr nonlinear medium and a linear absorber. The nonlinear medium is characterized with nonlinearity coefficient n_2, and the absorber is characterized with absorption coefficient α. Pump light is sent into the ring resonator through a coupling mirror. We assume that the light field inside the resonator includes carrier A and idler and signal sidebands B_+ and B_- respectively ($E = A\exp[-i(\omega t - kz)] + B_+\exp[-i(\omega_+ t - k_+ z)] + B_-\exp[-i(\omega_- t - k_- z)]$), $k = \omega n/c$, $k_\pm = \omega_\pm n/c$; and that only the optical carrier is pumped from outside $E_{in} = A_{in}\exp(-i\omega t)$.

medium, in- and out-coupling port, and a linear absorber. For the sake of simplicity, we neglect by the depletion of the pump wave, assuming that the total power of the generated fields is much less than the pump power. This is the case in the majority of experiments because the pump power generally exceeds the power of the sidebands tenfold or even more. A generalized theoretical study of a saturated hyperparametric oscillator based on three optical WGMs is reported in [18]. On the other hand, optical comb generation can be associated with soliton formation effects, so a theoretical study of the frequency stability of the saturated optical comb based on the four wave mixing in a WGM resonator is to be performed in the future.

The parametric amplifier is characterized with coefficient G (see Eqs. (2)-(4))

$$G = L\omega_0 n_2 \frac{\hbar\omega}{\mathcal{V} n}|A|^2, \tag{1}$$

where $L = 2\pi R$ is the length of the circumference of the resonator, R is the radius of the resonator, A is the slow amplitude operator of the pump field normalized such that $|A|^2$ describes number of pump photons in the mode of the resonator; n_2 stands for the Kerr nonlinearity of the material, n is the linear index of refraction of the material, $\mathcal{V}$ is the WGM volume. It worth to note that $G = gLn|A|^2/c$, where g is the coupling parameter introduced in the oscillator model discussed in [18].

Passing the amplifier (denoted as a triangle in Fig. 1) the pump wave experiences self phase modulation only

$$A_{Gout} = A_{Gin}e^{iG}, \tag{2}$$

where $A_{Gin} = |A_{Gin}|\exp i\phi_A$ and A_{Gout} characterize the pump amplitude at the entrance and exit of the amplifier inside the resonator. The signal and idler modes experience not only the phase shift, but also amplification

$$B_{Gout+} = \left[B_{Gin+} + iG(B_{Gin+} + B^*_{Gin-}e^{2i\phi_A})\right]e^{iG}, \tag{3}$$

$$B^*_{Gout-} = \left[B^*_{Gin-} - iG(B_{Gin+}e^{-2i\phi_A} + B^*_{Gin-})\right]e^{-iG}, \tag{4}$$

where B_+ and B_- are the slow amplitude operators of the idler and signal. Frequencies of the

#90022 - $15.00 USD Received 21 Nov 2007; revised 22 Feb 2008; accepted 22 Feb 2008; published 12 Mar 2008

generated sidebands (ω_+ and ω_-) obey to the energy conservation law

$$2\omega = \omega_+ + \omega_-, \tag{5}$$

To find the intracavity field E we write the additional condition for the field components resulting from the propagation of the light through the linear part of the resonator

$$A_{Gin} = A_{Gout} e^{i\omega Ln/c} e^{-\alpha} \sqrt{1-T_c} + \sqrt{T_c} A_{in}, \tag{6}$$

$$B_{Gin\pm} = B_{Gout\pm} e^{i\omega_\pm Ln/c} e^{-\alpha} \sqrt{1-T_c}, \tag{7}$$

where $\alpha \ll 1$ is the total light absorption in the resonator per round trip (does not depend on the frequency), $T_c \ll 1$ is the coupling factor. It is useful to remind that all but one (A_{in}) field parameters in Eqs. (6) and (7) belong to the intracavity fields.

Combining (2) and (6) we get equation for the optical pump

$$|A_{Gin}| e^{i\phi_A} \left\{ 1 - e^{i(G+\omega Ln/c)} e^{-\alpha} \sqrt{1-T_c} \right\} = \sqrt{T_c} A_{in}; \tag{8}$$

combining (3-4) and (7) we derive equations for the sidebands

$$B_{Gin+} \left[e^{-i\omega_+ Ln/c+\alpha} (1-T_c)^{-1/2} - (1+iG) e^{iG} \right] = iG e^{i(2\phi_A+G)} B^*_{Gin-}, \tag{9}$$

$$B^*_{Gin-} \left[e^{i\omega_- Ln/c+\alpha} (1-T_c)^{-1/2} - (1-iG) e^{-iG} \right] = -iG e^{-i(2\phi_A+G)} B_{Gin+}, \tag{10}$$

which result in the oscillation condition

$$\left[e^{-i\frac{\omega_+-\omega_-}{2}\frac{Ln}{c}+\alpha} - \sqrt{1-T_c} \right]^2 = e^{-i\frac{\omega_+-\omega_-}{2}\frac{Ln}{c}+\alpha} \sqrt{1-T_c} \left[e^{-i(\omega Ln/c+G)} (1-iG) + c.c. - 2 \right], \tag{11}$$

Deriving Eq. (11) we have used Eq.(5).

Eq.(11) can be decomposed into two equations

$$\exp\left[-i \frac{\omega_+ - \omega_-}{2} \frac{Ln}{c} \right] = 1, \tag{12}$$

$$\left[e^{\alpha} - \sqrt{1-T_c} \right]^2 = e^{\alpha} \sqrt{1-T_c} \left[e^{-i(\omega Ln/c+G)} (1-iG) + c.c. - 2 \right], \tag{13}$$

where (12) is the condition for the oscillation frequency, and (13) is the condition for the pump amplitude and frequency required to sustain the oscillations (c.f. Eq. B20 of [18]). Eq.(13) is to be solved together with Eq.(8), and then the amplitude of the output pump light A_{out} can be found from equation

$$A_{out} = -A_{Gin} e^{i(G+\omega Ln/c)} e^{-\alpha} \sqrt{T_c} + A_{in} \sqrt{1-T_c}: \tag{14}$$

$$A_{out} = \frac{\sqrt{1-T_c} - \exp[i(G+\omega Ln/c)] \exp[-\alpha]}{1 - \exp[i(G+\omega Ln/c)] \exp[-\alpha] \sqrt{1-T_c}} A_{in} \tag{15}$$

We derive the oscillation threshold conditions from Eq.(13)

$$-i \left(e^{-i\omega Ln/c} - 1 \right) \simeq 2 \left(\alpha + \frac{T_c}{2} \right), \tag{16}$$

$$G \simeq \alpha + \frac{T_c}{2}. \tag{17}$$

#90022 - $15.00 USD Received 21 Nov 2007; revised 22 Feb 2008; accepted 22 Feb 2008; published 12 Mar 2008

The conditions mean that the oscillation start when the gain approaches the absorption, and that the detuning of the pump laser from the resonance should be specially selected for the oscillations to start. The frequency of the drive field (16) is selected such that G reaches its absolute minimum at that point. This frequency tuning slightly differs from the tuning corresponding to the smallest value of the outside optical pumping that results in reaching the oscillation threshold [18].

We find from (12) that

$$\omega_+ - \omega_- = \frac{2c}{Rn} = 2\Omega_{FSR}. \tag{18}$$

The frequency difference of the generated field depends on the natural free spectral range (FSR) of the resonator only. There is no dependence on the cross- and self-phase modulation effects. It confirms our previous conclusion that the nonlinear effects do not influence the oscillation frequency if one considers a completely symmetric three mode model of the oscillator [18]. Influence of the effects on the noise of slightly asymmetric systems as well as systems containing many modes (optical combs) is to be studied. We have neglected the material as well as geometrical dispersion in the above analysis. However this rule holds even for a dispersive resonator [18]. Keeping in mind Eq. (5), we find that the generated sidebands are always equidistant

$$\omega_+ - \omega = \omega - \omega_- = \Omega_{FSR}. \tag{19}$$

Eqs. (9) and (10) do not provide information on the steady state of the sideband amplitude, however they carry information about relative phase and amplitude of the sidebands. Using Eq. (19) we find that

$$e^{i\omega Ln/c} = e^{i\omega_\pm Ln/c}. \tag{20}$$

Substituting Eq. (20) into Eqs. (9) and (10) and using Eq. 13 we obtain

$$|B_{Gin+}| = |B_{Gin-}|, \tag{21}$$

i.e. we find that the generated signal and idler sidebands have equal amplitudes. Defining phases of the sidebands as $B_{Gin\pm} = |B_{Gin\pm}| \exp i\phi_\pm$ we obtain from Eqs. (9) and (10) that far above the threshold ($G \gg T_c/2 + \alpha$)

$$e^{i(2\phi_A - \phi_- - \phi_+)} \simeq -\frac{\sqrt{G^2 - (\alpha + T_c/2)^2} + i(\alpha + T_c/2)}{G} \simeq -1, \tag{22}$$

while for the pump light we have (in accordance with (15))

$$A_{out} \simeq \frac{\alpha - T_c/2 - i(\sqrt{G^2 - (\alpha + T_c/2)^2} - G)}{\alpha + T_c/2 - i(\sqrt{G^2 - (\alpha + T_c/2)^2} - G)} A_{in}, \tag{23}$$

which approaches $-A_{in}$ if $T_c/2 \gg \alpha$ (overcoupled resonator). Combining Eq. (21), (22), and (23) we conclude that the light exiting the resonator is nearly phase modulated

$$|B_+ A^*_{out} + A_{out} B^*_-|^2 \to 0, \quad \text{if} \quad G \gg T_c/2 + \alpha. \tag{24}$$

It is possible to show that the modulation type does not change if one uses a resonator with two couplers instead of one coupler. The phase modulation should be converted to the amplitude modulation to observe the modulated signal by means of a fast photodiode. Such a conversion can be realized using an optical filter or a local oscillator.

The basic results of the section are: (i) we have shown that the hyperparametric oscillations occur as the result of self- and cross-phase modulation in a dielectric material possessing Kerr nonlinearity, (ii) the light escaping the nonlinear resonator is mostly phase modulated if the resonator is overcoupled.

#90022 - $15.00 USD Received 21 Nov 2007; revised 22 Feb 2008; accepted 22 Feb 2008; published 12 Mar 2008

2.2. Noise

Let us discuss now the phase noise of the hyperparametric oscillator based on the nonlinear WGM resonator. The light escaping the resonator is phase modulated, as is shown above. Therefore, the slow amplitude of electric field at the exit of the resonator (Fig. 2) can be represented as

$$E_{out} = A + 2iB\sin[\omega_M t + \phi(t)], \tag{25}$$

where B is the amplitude of each sideband, ω_M is the frequency difference between the generated sidebands and the pumping light, and $\phi(t)$ is the oscillator phase noise. With the appropriate choice of the origin of time, we can assume that A and B are real. The field amplitude at the photodiode is

$$E_{PD} = E_{out}e^{-\alpha_{c2}}r + E_{LO}e^{i\psi_{LO}}\sqrt{1-r^2}, \tag{26}$$

where $e^{-\alpha_{c2}}$ is the amplitude loss at the output coupler (Cp2), E_{LO} is the amplitude of the electric field of the local oscillator (we use the local oscillator to transform the phase modulation into the amplitude modulation), ψ_{LO} is the phase of the local oscillator, r is the amplitude transmissivity of the splitter Sp2. We select $\psi_{LO} = \pi/2$, then the DC optical power on the photodiode is

$$P_{PD} = P_A e^{-2\alpha_{c2}}r^2 + P_{LO}(1-r^2), \tag{27}$$

where P_A is the power of optical carrier escaping the resonator, and P_{LO} is the power of the local oscillator.

The AC photocurrent in the photodiode is given as

$$j = 4\mathscr{R}E_{LO}Be^{-\alpha_{c2}}\sqrt{1-r^2}\sin[\omega_M t + \phi(t)], \tag{28}$$

where $\mathscr{R}$ is the responsivity of the photodiode; so that the demodulated time averaged microwave power is

$$P_{mw} = 8\rho\mathscr{R}^2 P_{LO}P_B e^{-2\alpha_{c2}}(1-r^2), \tag{29}$$

where ρ is the resistance at the output of the photodiode.

The phase noise of the oscillator can be described by a modified Leeson formula [25]

$$S_\phi \simeq \left[1 + \frac{\eta P_{mw}}{2\rho\mathscr{R}^2 P_{PD}^2}\frac{P_{PD}}{P_B}\frac{\gamma^2}{f^2}\right]\frac{2h\nu_0}{\eta P_{PD}} \simeq \left[1 + 4\eta e^{-2\alpha_{c2}}\frac{\gamma^2}{f^2}\right]\frac{2h\nu_0}{\eta P_{LO}(1-r^2)}, \tag{30}$$

where γ is the half width of the half maximum of the loaded WGM resonance and ν_0 is the carrier frequency, η is the quantum efficiency of the detector. The first term in the right hand side stands for the shot noise, and the second – for the noise associated with the phase diffusion. The Leeson formula was originally developed for electronic oscillators [25]. As one can see, the phase noise of the photonic microwave oscillators can be described by means of similar relationship. We have taken into account that the phase diffusion of the unsaturated oscillator is determined by the optical sideband power P_B [18], similarly to the Schawlow-Townes linewidth [26],

$$D_\phi \simeq \frac{(2\pi\gamma)^2}{4}\frac{h\nu_0}{P_B}, \tag{31}$$

and that the corresponding phase noise spectral density is

$$S(f) = \frac{4D_\phi}{(2\pi f)^2}. \tag{32}$$

It is interesting to note that the Leeson frequency is equal to γ in a conventional microwave oscillator [24], but it is twice less than γ in the hyperparametric oscillator (see Eq. (31)) because

#90022 - $15.00 USD Received 21 Nov 2007; revised 22 Feb 2008; accepted 22 Feb 2008; published 12 Mar 2008

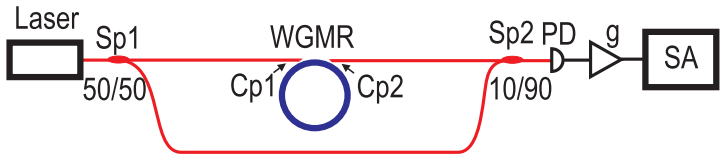

Fig. 2. Experimental setup. Light from a YAG laser is split at a 50/50 splitter Sp1. One part is sent into a CaF_2 WGM resonator (WGMR) through coupler Cp1. The other part is sent to a fiber delay line. The light is retrieved out of the resonator using the coupler Cp2, is combined with the light propagated through the delay line using splitter Sp2, and sent to the fast photodiode (PD). About 90% of light from the resonator goes to the photodiode. Microwave signal at the output of the photodiode is preamplified with an amplifier (g) and forwarded to a microwave spectrum analyzer (SA).

the oscillator generates two correlated harmonics. This value can be even less if the oscillator generates an optical comb. The corner frequency of the phase noise, determined as the frequency at which the white shot noise and the oscillator phase diffusion noise equally contribute to the phase noise, (30) can be different from the Leeson frequency depending on the residual absorption in the fiber link and the coupling losses.

The basic conclusions of the theoretical consideration is that (i) the power spectral density of the phase noise of the oscillator does not depend on the efficiency of the parametric process, but the generated microwave power is proportional to the power of the optical sidebands; and (ii) the corner frequency of the phase noise can exceed the half width of the half maximum of the loaded WGM resonance. As will be shown below, these conclusions are consistent with our experimental observations.

3. Experiment

In our experiments light from a YAG laser was sent into a CaF_2 WGM resonator and retrieved out of the resonator using two angle cut fiber couplers Cp1 and Cp2 (Fig. 2). The laser linewidth was less than 5 kHz, and the maximum coupling efficiency was better than 50%. A typical CaF_2 resonator had a toroidal shape with a diameter of several millimeters and thickness in the range of several hundred microns (the preform thickness had 500 μm thickness). The resonator loaded Q-factor was on the order of 10^9 (intrinsic Q-factor exceeded 10^{10}).

The resonator starts to oscillate generating signal and idler sidebands when the optical pumping power exceeds some threshold value (typically a milliwatt). We found that if the light emerging from the resonator is directly sent to a photodiode it does not generate any detectable microwave signal. However the modulation appears if the resonator is placed into an arm of a Mach-Zehnder interferometer and the delay in the second arm of the interferometer is correctly chosen. This is a distinct property of phase modulated light. A typical picture of phase noise of the generated microwave signal is shown in Fig. (3). The lowest noise floor we observed was -126 dBc at 300 kHz.

We have performed a more careful study of the oscillator noise properties. The basic conclusions are that (i) the noise floor of the oscillator is shot noise limited if the length of the delay line is properly selected so as the delay does not act as the discriminator to the laser frequency noise, and (ii) that the Leeson frequency exceeded the half width of the half maximum of the loaded WGM resonance. The results of the measurements are presented in Figs. (4) and (5).

Let us show that the observed phase noise is limited by the shot noise. The shot noise is $S_j = 2q\overline{j}$ (A^2/Hz), where $\overline{j} = \mathscr{R}\overline{P}_D$ is the photocurrent, $\overline{P}_D = 6\times10^{-3}$ W is the average optical

#90022 - $15.00 USD Received 21 Nov 2007; revised 22 Feb 2008; accepted 22 Feb 2008; published 12 Mar 2008

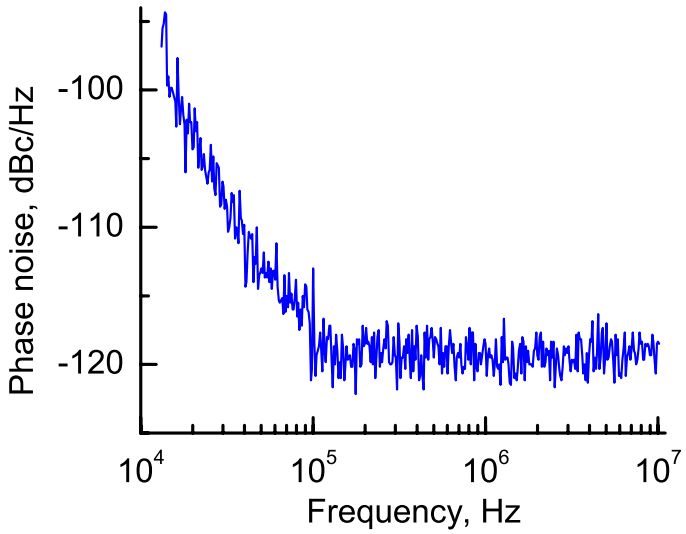

Fig. 3. Typical phase noise of the oscillator. The loaded quality factor of the resonator is $Q \simeq 10^9$, so that half width at the half maximum of the resonance is $\gamma \simeq 115$ kHz. The length of the delay line is ~ 115 m. This is shorter length compared with the length of the delay line that corresponds to $Q = 10^9$ (~ 300 m), however the delay line gave us the best overall oscillator performance. The total optical power on the detector PD is 6 mW. The power of the microwave signal leaving the detector is -46.1 dBm. The output microwave amplifier has an estimated 7 dB noise figure and 43.1 dB of gain. The power of the output microwave signal at the spectrum analyzer is -3 dBm.

power, $\mathscr{R} = \eta q/\hbar\omega = 0.8$ A/W is the responsivity of our detector at $\lambda = 1320$ nm, and η is the quantum efficiency of the detector. Introducing the load resistance ρ (50 Ohm in our case) at the detector output, the shot noise spectrum is

$$S_{shot} = 2q\mathscr{R}\overline{P}_D\rho = 7.7\times10^{-20}\mathrm{W/Hz} \quad (-161\ \mathrm{dBm/Hz}),$$

The thermal noise spectrum is

$$S_{thermal} = kT = 4\times10^{-21}\mathrm{W/Hz} \qquad (-174\ \mathrm{dBm/Hz}).$$

The detector output is only accessible through the microwave amplifier, which adds its noise. The latter is specified as the noise figure F, which includes thermal noise at the standard temperature $T_0 = 290$ K (17 °C). Thus, we replace kT with FkT_0. We neglect the difference between T_0 and the actual room temperature. The background of the readout system, detector and amplifier, converted into phase noise is

$$S_\phi = \frac{S_{shot} + S_{ampli}}{P_{mw}|_D} = \frac{2q\mathscr{R}\overline{P}_D\rho + FkT_0}{P_{mw}|_D} = \frac{2q\mathscr{R}\overline{P}_D\rho + FkT_0}{P_{mw}|_{SA}/g^2},$$

where P_{mw} is the demodulated averaged microwave power at the detector output or at the spectrum analyzer input, and g^2 is the amplifier power gain. The quantity $\mathscr{L}(f)$, defined as $\mathscr{L}(f) = \frac{1}{2}S\phi(f)$, is the most commonly used in the literature [27].

#90022 - $15.00 USD Received 21 Nov 2007; revised 22 Feb 2008; accepted 22 Feb 2008; published 12 Mar 2008

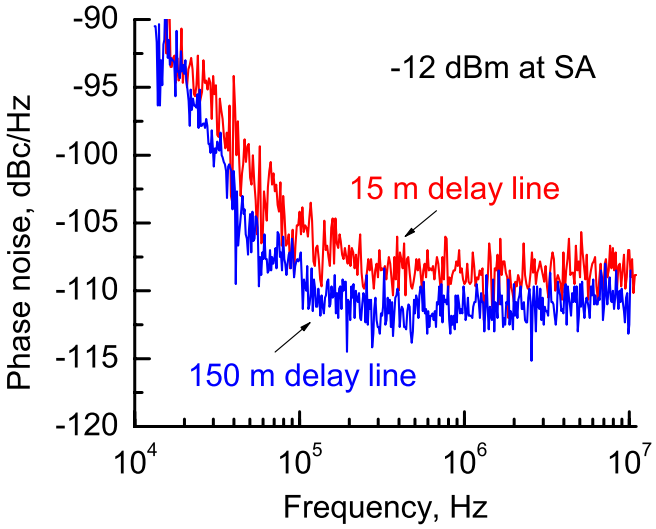

Fig. 4. Phase noise of the oscillators with different lengths of the delay line. The quality factor of the resonator is $Q \simeq 10^9$. The optical power at the detector is 6 mW. The power of the output microwave signal at the spectrum analyzer is -12 dBm. The output microwave amplifier has an estimated 15 dB noise figure and 35 dB of gain. The noise decreases when the group delay of the resonator approaches the delay of the fiber link.

The above evaluates as $S_\phi = 3.9\times10^{-12}$ rad^2/Hz ($\mathscr{L} = -117$ dBc/Hz) with $\overline{P}_D = 6\times10^{-3}$ W, $g^2 = 2\times10^4$ (43 dB), $F = 5$ (7 dB), and $P_{mw}|_{SA} = 5\times10^{-4}$ W (-3 dBm). This calculated floor is some 2 dB higher than the floor shown in Fig. 3. This small discrepancy can result from measurement uncertainty, or be the signature of the noise.

We have observed linear increase of the phase noise floor of the microwave signal versus the light power on the photodiode. However, the phase noise does not appear flat in all the measurements (see, e.g., Fig. 4), which one would expect in the case of shot noise limited operation. More rigorous studies of the oscillator noise are required.

The thermal noise considered in the paper is related to the photodetector as well as the microwave circuit. We had not taken into account the fundamental thermodynamic noises influencing the stability of the microwave signal. Those noises are orders of magnitude smaller compered with the observed noises, in accordance with the theoretical predictions [11, 12]. However, the situation can change if one will use small resonators where the thermodynamic noise increases.

Therefore, our experiment confirms that the phase noise floor of the hyperparametric oscillator agrees with shot noise limited operation and that the corner frequency of the power spectral density of the phase noise is determined by the linewidth of the WGM resonances. Increase of the quality factor of the resonator will result in an improvement of the oscillator properties. Generation of multiple harmonics also should be profitable.

#90022 - $15.00 USD Received 21 Nov 2007; revised 22 Feb 2008; accepted 22 Feb 2008; published 12 Mar 2008

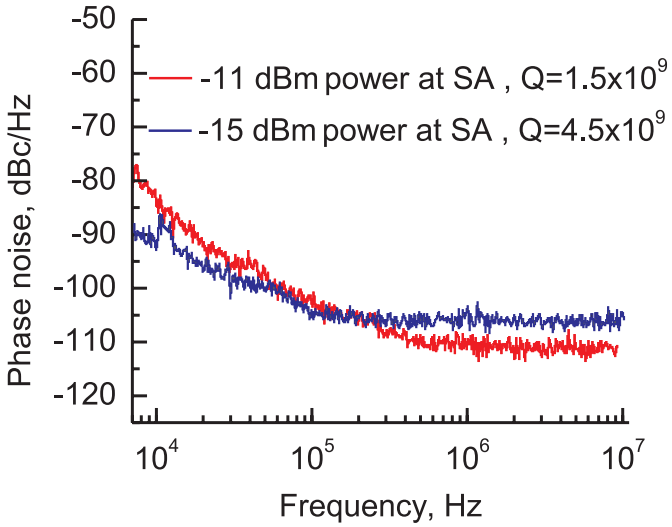

Fig. 5. Phase noise of the microwave signal as a function of the Q. The Q was changed by controlling the loaded coupling to the resonator. The higher Q value was achieved with a smaller loading. It results in a smaller corner frequency, but also in a larger noise floor. Noise floor rises because the higher Q corresponds to the bigger insertion loss in the resonator. On the other hand, the higher Q results in more efficient nonlinear process and increase of the generated sideband that reduces the phase diffusion of the oscillator.

4. Dispersive properties of calcium fluoride WGM resonators and prospects for optical comb generation

4.1. Dispersion of WGMs: theory

The maximum possible frequency between the signal and idler fields in our experiment is determined by the nonequidistance of the modes of the resonator, occurring because of the second order dispersion of the material and the geometrical dispersion given by the mode structure. We introduce a parameter $D = (2\nu_0 - \nu_+ - \nu_-)/2\gamma$ to characterize the total dispersion, where ν_0, ν_+, and ν_- are the frequencies of the pump, idler, and signal modes respectively. If $|D| \geq 1$ the modes of the resonator are essentially not equidistant and the oscillations are suppressed due to the energy conservation law. Using Sellmeier's dispersion equation for CaF_2 we find $D \sim 0.05$ at 1.3 μm laser wavelength and $Q = 10^9$ in our resonator. This implies that the maximum number of sidebands generated in our WGM resonator made of fluorite does not exceed 200. Generation of a larger number of harmonics is possible but different pump frequency or lower Q resonator is required. We do not observe generation of multiple harmonics because of the efficient Raman scattering that masks the oscillations at higher pump powers, as well as because of the change of the mode spacing due to the interaction between WGM in the resonator.

The geometrical dispersion of the WGM resonator is normal. This means that longer wavelength pulses travel faster in the resonator. This might be explained by the fact that longer wavelength modes are located deeper in the interior of the resonator and, therefore, their geometrical length is shorter. The material dispersion, which can be negative, together with the geometrical dispersion of the resonator can result in a positive as well as a negative group ve-

#90022 - $15.00 USD Received 21 Nov 2007; revised 22 Feb 2008; accepted 22 Feb 2008; published 12 Mar 2008

locity dispersion [28]. It is also possible to achieve $D = 0$ for a given resonator and achieve generation of a large multiple of harmonics (comb) [14].

Let us estimate the width of the optical comb that can be generated in the oscillator. The WGM spectrum is described by

$$\frac{n(\omega_l)}{c}\omega_l \simeq \frac{l}{R}\left[1+\frac{1.86}{l^{2/3}}\right], \tag{33}$$

where $l \gg 1$ is the mode number, R is the radius of the resonator, $n(\omega_l)$ is the index of refraction of the material for mode frequency ω_l. The frequency dependence of the index of refraction can be presented in the form

$$\frac{\omega_l}{c}n(\omega_l) \simeq \frac{\omega_{l0}}{c}n(\omega_{l0}) + \beta'(\omega_{l0})[\omega_l-\omega_{l0}] + \frac{1}{2}\beta''(\omega_{l0})[\omega_l-\omega_{l0}]^2 + \frac{1}{6}\beta'''(\omega_{l0})[\omega_l-\omega_{l0}]^3, \tag{34}$$

where β-parameters characterize the dispersion of the medium, and ω_{l0} is some fixed frequency. We select ω_{l0} such that

$$\beta''(\omega_{l0}) \simeq -\frac{R[\beta'(\omega_{l0})]^2}{l^{5/3}}, \tag{35}$$

so that ω_{l0} corresponds to the point of zero quadratic dispersion of the resonator [28]. In this case

$$[\omega_{l0+\mu+1}-\omega_{l0+\mu}] = [\omega_{l0+1}-\omega_{l0}] + \mu^2\frac{2[\beta''(\omega_{l0})]^2-\beta'''(\omega_{l0})\beta'(\omega_{l0})}{2R^3[\beta'(\omega_{l0})]^5}, \tag{36}$$

and the spectral width of the comb ($2\mu[\omega_{l0+\mu+1}-\omega_{l0+\mu}]$) can be estimated from expression $[\omega_{l0+\mu+1}-\omega_{l0+\mu}]-[\omega_{l0+1}-\omega_{l0}] = 2\pi\gamma$, or

$$\Delta\omega_{comb} = \frac{\beta'(\omega_{l0})}{\mathscr{F}^{1/2}}\left\{2[\beta''(\omega_{l0})]^2-\beta'''(\omega_{l0})\beta'(\omega_{l0})\right\}^{-1/2}, \tag{37}$$

where $\mathscr{F} = 2\pi\gamma R\beta'(\omega_{l0})$ is the finesse of the resonator. We have found that, for example, for a resonator with $Q = 10^{10}$ and $FSR = 10$ GHz the generated comb can be as wide as $\Delta\omega_{comb} = 2\pi\times 6.5$ THz; a decrease in quality factor to $Q = 10^8$ results in broadening of the comb to 65 THz. This value is close to the width of the comb observed in fused silica resonators [14].

4.2. Dispersion of WGMs: measurement

We have studied the dispersive properties of CaF_2 using a toroidal resonator with $R \simeq 0.35$ cm ($FSR = 9.438$ GHz) and $Q \simeq 10^9$. The results of our measurements are shown in Fig. 6. We also have drawn there the theoretical dependencies of the dispersion obtained from Sellmeier's dispersion equation [29] for the bulk material as well as the resonator. It is easy to see that there is a significant discrepancy between the measurement results and theoretical predictions. The reason could be (i) variation of the dispersion properties of the material compared with the properties of the sample used for derivation of the Sellmeier's dispersion equation, (ii) not enough accuracy in the measured FSR of the WGM resonator, (iii) interaction among various WGM families. The good news is that the zero dispersion point for CaF_2 is in the vicinity of the telecom optical frequency.

The experimental setup for the dispersion measurement is shown in Fig. (7). Light from a white light source (WLS, approximately 30 nm bandwidth) was filtered out with a widely tunable optical pass-band filter having approximately 1 nm linewidth. The portion of the light that passed the filter was sent to a WGM resonator (MRA) using a coupling prism. The light was interacting with approximately a dozen of WGM modes belonging to the main mode family as

#90022 - $15.00 USD Received 21 Nov 2007; revised 22 Feb 2008; accepted 22 Feb 2008; published 12 Mar 2008

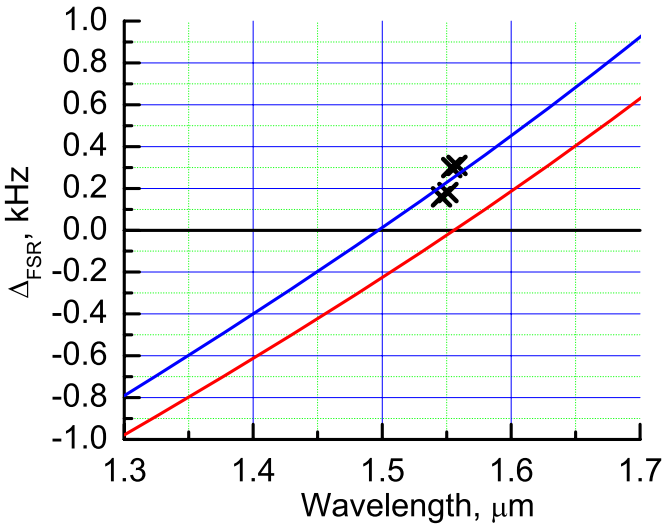

Fig. 6. Dispersion of CaF_2 resonator shown as the dependence of difference between frequencies of two adjacent FSRs vs. the wavelength. The resonator has an average $FSR \simeq 9.44$ GHz. Solid lines correspond to the dependencies derived from the corresponding Sellmeier's equation. Blue line stands for the bulk material dispersion, red line – for the resonator dispersion (geometrical and material). The red line shifts to the right for smaller resonators.

well as with multiple other modes of the resonator. We interrogated the WGMs using another prism coupler. The light exiting this coupler was sent to a fast photodiode (PD). The resultant RF signal from the photodiode was amplified with amplifier (A) and sent to a stabilized RF spectrum analyzer (SA). The frequency of the RF signal shows FSR averaged among several WGMs.

An example of the measured RF signal is shown in Fig. (8). We assumed that the maximum signal belongs to the basic mode sequence and measured its position. The central frequency of the filter was shifted after the measurement was completed and the measurement procedure was repeated with new filter position. The overall accuracy of the measurement is on the level of several kHz. The basic disadvantage of the measurement strategy is the uncertainty while making connections between RF and optical spectra.

4.3. Advantages of an optical comb for microwave photonics applications

The optical comb is particularly interesting for the photonic generation of microwaves because it results in a substantial reduction of the noise of the generated signal. The noise reduction is most pronounced in stabilized equidistant combs and can be explained as an efficient frequency division of the optical frequency [8]. We assume that the comb has N optical harmonics. If any two optical frequencies separated by N comb FSRs are mutually stable, and the comb harmonics are phase locked and essentially equidistant, the phase noise of the beatnote of any two neighboring harmonics is N times lower than the noise of the optical frequencies [8].

The output microwave power has a saturation point when an optical comb is used to generate

#90022 - $15.00 USD Received 21 Nov 2007; revised 22 Feb 2008; accepted 22 Feb 2008; published 12 Mar 2008

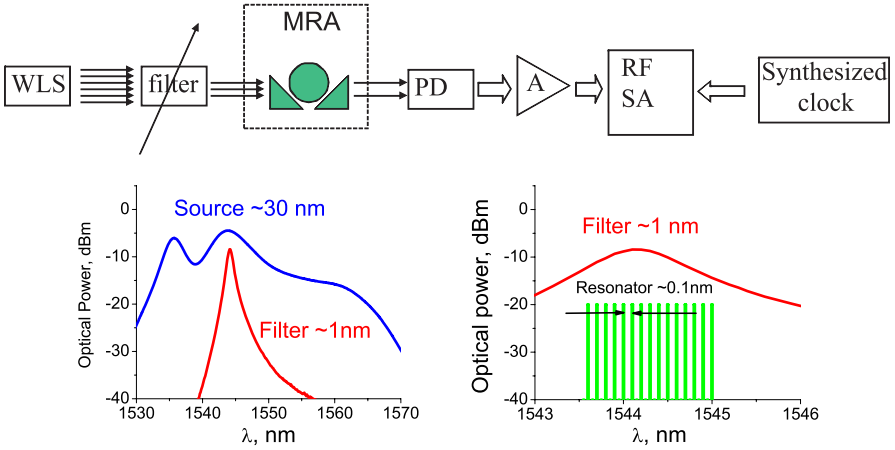

Fig. 7. Setup for measurement of the dispersion of CaF_2 resonator.

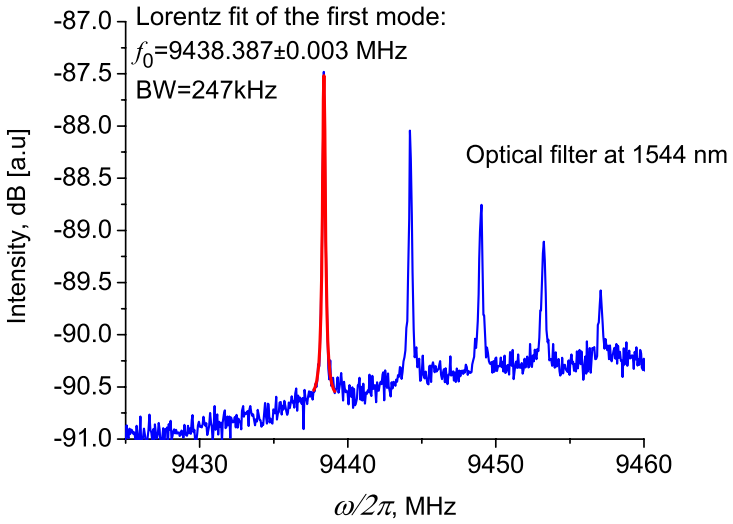

Fig. 8. Preamplified microwave signal measured using an RF spectrum analyzer.

#90022 - $15.00 USD Received 21 Nov 2007; revised 22 Feb 2008; accepted 22 Feb 2008; published 12 Mar 2008

microwave signals. If the electric field of the optical comb is

$$E = e^{-i\omega_0 t} \sum_{k=1}^{N} E_k e^{-i(k-1)\omega_M t}, \tag{38}$$

then the power of microwaves radiation with frequency ω_M generated at the photodiode is given by beating of neighboring harmonics

$$P_{mw} \sim |\sum_{k=1}^{N} E_k^* E_{k+1}|^2. \tag{39}$$

Assuming that the power of each optical harmonic is $P_k = P_0/N$, we find

$$P_{mw} \sim P_0^2, \tag{40}$$

in other words, the maximal generated microwave power does not depend on the number of the comb harmonics. This maximum is achievable for a comb possessing "amplitude modulation nature" only because the interference of the harmonics occur on the photodiode only if components $E_k^* E_{k+1}$ have the same phase. For a "phase modulated comb", for example, $\sum_{k=1}^{N} E_k^* E_{k+1} = 0$ and no microwave signal can be detected.

5. Discussion

One of the basic experimental challenges for the demonstration of a low noise hyperparametric oscillator is related to the stimulated Raman scattering (SRS) that adds to the noise of the microwave signal. The SRS starts right after the hyperparametric oscillations when the power of the first signal and idler sidebands are at the level of several tens of microwatt (several percents of the overall optical power entering the resonator), and the microwave signal becomes noisy as the SRS process develops. Raman process is efficient because modes corresponding to Stokes light generally have higher quality factors. The Stokes light is generated in different mode families uncoupled from the fiber couplers. The solution to this problem is in the fabrication of WGM resonators of a proper shape, or usage of special geometrical/spectral dampers to decrease the SRS efficiency. Suppression of the SRS process will lead to an increase in the number of the optical sidebands without adding noise to them. We expect that this broadening of the optical comb will further improve the noise properties of the generated microwave signal. The number of the optical harmonics is inversely proportional to the square root of the finesse of the resonator and phase diffusion of the microwave signal is inversely proportional to the finesse, so we anticipate that the noise properties will still be improved if one increases the finesse of the resonator.

6. Conclusion

We have studied properties of a hyperparametric microwave oscillator based on a calcium fluoride whispering gallery mode resonator, and have shown that the oscillator is promising for generation of high frequency low noise microwave signals. We have also identified the limitations to the spectral purity obtained in our work, and shown approaches that can improve the observed performance of the hyperparametric oscillator.

Acknowledgment

The research described in this paper was supported by DARPA.

#90022 - $15.00 USD Received 21 Nov 2007; revised 22 Feb 2008; accepted 22 Feb 2008; published 12 Mar 2008